

Intraply and interply hybrid composites based on E-glass and poly(vinyl alcohol) woven fabrics: tensile and impact properties

Alessandro Pegoretti,^{1*} Elena Fabbri,² Claudio Migliaresi¹ and Francesco Pilati²

¹Department of Materials Engineering and Industrial Technologies, University of Trento, via Mesiano 77, 38050 Trento, Italy

²Department of Materials and Environmental Engineering, University of Modena and Reggio Emilia, via Vignolese 905, 41100 Modena, Italy

Abstract: E-glass and poly(vinyl alcohol) (PVA) fibres were used to produce both homogeneous and hybrid composites with an orthophthalic unsaturated polyester resin. Results are presented regarding the tensile and impact behaviour of both intraply and interply hybrid composites, with particular regard to the effects of the plies stacking sequence and the loading direction. With a proper choice of composition and stacking sequence, E-glass/PVA hybrid composites were proved to achieve a property profile superior to those of homogeneous E-glass laminates in terms of specific properties. In particular, hybridization with PVA fibres resulted in improving the specific impact energy of E-glass laminates. Resistance to impact crack propagation was higher for intraply with respect to interply hybrid composites, as evidenced by their ductility index values.

© 2004 Society of Chemical Industry

Keywords: mechanical properties; hybrid; glass fibres; poly(vinyl alcohol) fibres

INTRODUCTION

Composites containing two or more different reinforcing materials bound in the same matrix are commonly known as hybrid composites. Hybridization allow designers to tailor the composite properties to the exact needs of the structure under consideration.^{1–5} In most cases, the purpose of hybridization is to obtain a new material retaining the advantages of its constituents, and hopefully overcoming some of their disadvantages. Another desired achievement is related to the cost, with one of the two components being generally cheaper than the other one. There are several types of hybrid composites,^{4,5} depending on the way the constituent materials are mixed, ie: (i) interply hybrids where layers of the two (or more) homogeneous reinforcements are stacked; (ii) intraply hybrids in which tows of the two (or more) constituent types of fibres are mixed in the same layer; (iii) intimately mixed (intermingled) hybrids where the constituent fibres are mixed as randomly as possible so that no concentrations of either type are present in the material; (iv) selective placement in which reinforcements are placed where additional strength is needed, over the base reinforcing laminate layer; (v) superhybrid composites which are composed of metal foils or metal composite plies stacked in a specified orientation and sequence.

The diversity of the properties and the possible material combinations are too numerous to detail here. As far as polymer matrix composites are concerned, most of the available literature data refer to carbon/glass,^{6–12} carbon/Kevlar^{12–17} and carbon/ultra-high-modulus-polyethylene (UHMPE)^{17–25} fibre-reinforced hybrids, with the main purpose being to improve the energy-absorbing capability of carbon fibres. Other hybrid systems recently investigated are based on carbon/nylon,¹⁷ aramid/UHMPE^{17,26,27} and UHMPE/glass²⁸ biofibre (pineapple leaf, sisal, bamboo fibres)/glass.^{29–32} Sometimes, a 'hybrid effect', briefly defined as a positive deviation of a certain property from the 'rule of mixtures', have been reported.^{33,34} With respect to the tensile behaviour, the hybrid effect is generally defined as an enhancement of the first failure strain of the low-elongation fibre-reinforced component. In many cases, an improvement in the specific ultimate properties of polymer composites with inorganic brittle reinforcements such as carbon or glass fibres was attempted^{14,18–25} by the incorporation of more ductile organic fibres, such as aramid or UHMPE.

Recent developments in the field of high-performance organic fibres have been mainly directed toward the achievement of elevated strength and modulus values via molecular orientation and chain extension of semi-rigid³⁵ or flexible macromolecules.³⁶

* Correspondence to: Prof Alessandro Pegoretti, Department of Materials Engineering and Industrial Technologies, University of Trento, via Mesiano 77, 38050 Trento, Italy

E-mail: Alessandro.Pegoretti@ing.unitn.it

(Received 31 July 2003; revised version received 20 October 2003; accepted 10 November 2003)

Published online 1 June 2004

At the same time, however, the transversal properties are reduced, being controlled by the secondary bonds between the oriented polymer chains, such as hydrogen bonding for aramid fibres, or van der Waals bonding in the case of UHMPE fibres. In order to overcome this limitation, the techniques of solution (gel)-spinning were applied to other, more polar, flexible polymers, such as polyamides, polyacrylonitrile, polyesters, and poly(vinyl alcohol) (PVA), even if the resulting modulus and strength values were rather low.³⁷⁻⁴¹ Some interesting results were obtained for PVA fibres, with a tensile modulus of up to 70 GPa and a stress at break of up to 2.3 GPa.³⁷⁻⁴⁰ Although the maximum tensile modulus and strength values are lower than in the case of UHMPE fibres, some advantages with respect to 'off-axis' and the long-term properties of PVA-based composites were confirmed,^{37,38} as expected from the specific intermolecular interactions (ie hydrogen bonds).

The objective of this present study is to evaluate a commercially available high-strength PVA fibre as a reinforcing material for applications in hybrid composites. Results are presented regarding the tensile and impact mechanical properties of E-glass/PVA fibres intraply and interply hybrid composites, with particular regard to the effects of the plies stacking sequence in different loading directions.

EXPERIMENTAL

Materials

The fabrics used for composite manufacturing were realized with the following fibres:

E-glass, type 111AX8 from Owens Corning Fiberglass, USA ($\rho = 2540 \text{ kg m}^{-3}$, $E_L = 73.0 \text{ GPa}$, $E_T = 73.0 \text{ GPa}$, $\sigma_b = 2000 \text{ MPa}$, $\varepsilon_b = 4.0 \%$); poly(vinyl alcohol) (PVA), Vinyon HM1 from Unitika Kasei Ltd, Japan ($\rho = 1270 \text{ kg m}^{-3}$, $E_L = 29.0 \text{ GPa}$, $E_T = 5.0 \text{ GPa}$, $\sigma_b = 1400 \text{ MPa}$, $\varepsilon_b = 6.0 \%$). (In the above, ρ is the density, E_L the longitudinal modulus, E_T the transverse modulus, σ_b the longitudinal tensile strength, and ε_b the longitudinal strain at break.)

All fabrics were fabricated and provided by Fibre e Tessuti Speciali Srl, Turin, Italy (FTS) in the form of both homogeneous and hybrid plain type fabrics. In particular, three different types of fabric were used, namely, a homogeneous E-glass fabric, a homogeneous PVA fabric and a hybrid E-glass/PVA fabric. More details about the composition of each

fabric are reported in Table 1. An orthophthalic unsaturated polyester (UP) resin, Sirester[®] FS 0995, provided by SIR Industriale Spa (Milan, Italy), was used as a matrix. The initial styrene content was about 39 wt%, methyl ethyl ketone peroxide (about 1.5 wt%) was added as the catalyst, the accelerator was cobalt octoate (about 0.2 wt%), and hydroquinone (about 0.15 wt%) was chosen as the inhibitor. The cured resin showed the following properties: $\rho = 1230 \text{ kg m}^{-3}$, $E_L = E_T = 3.5 \text{ GPa}$, $\sigma_b = 65 \text{ MPa}$ and $\varepsilon_b = 2.2 \%$.

Sample preparation

All composites consisted of four-ply laminates prepared by impregnating each fabric with the mixed UP resin by means of a hand roller. Composites were laminated in order to achieve various stacking sequences, as depicted in Figure 1. In particular, three types of laminates were obtained: (i) intraply hybrids (laminates A, B, C, D) in which both E-glass and PVA fibres are combined in the same layer; (ii) interply hybrids (laminates I, L, M, N) where single layers consist entirely either of E-glass or PVA fibres; (iii) homogeneous (laminates P, Q). With reference to Figure 1, samples are identified with a letter, indicating the laminate type, and a number, indicating the test direction. For example, sample A1 is obtained from laminate type A, with the longitudinal axis directed along direction 1.

The four-ply composites were then degassed for 30 s in a vacuum oven and placed in a stainless-steel mould whose surfaces were previously treated with a release agent. The minimum distance between the upper and lower mould plates was fixed at 2 mm. The mould was then placed between the plates of a hot press and all laminates were cured for 2 h at 50 °C, followed by 2 h at 100 °C under a constant pressure of 0.6 MPa. After shutting off the hot-press heaters, the mould was allowed to slowly cool down to room temperature under pressure before removing the laminate. These curing conditions provided fully cured laminates as confirmed from differential scanning calorimetry analysis. The resulting laminates were in the form of square plates (200 × 200 mm²) whose average thickness was in the range 1.44–1.97 mm depending on the composition (see Table 2). Rectangular specimens were machined from the laminates by using an air-cooled diamond disc saw.

Table 1. Composition of the various plain weave fabrics used for composite manufacturing

Fabric	Mass per unit area (kg m ⁻²)	Density (kg m ⁻³)	Fibre type		Fibre distribution (vol%)		Fibre yarn linear weight (dTex)		Fibre yarn count (yarn cm ⁻¹)	
			Warp	Weft	Warp	Weft	Warp	Weft	Warp	Weft
E-glass, homogeneous	0.374	2540	E-glass	E-glass	50	50	3200	3200	6	6
PVA, homogeneous	0.211	1270	PVA	PVA	68.4	31.6	3600	1800	4	3.7
E-glass/PVA hybrid	0.379	1660	PVA	E-glass	66.1	33.9	3600	3200	5.2	6

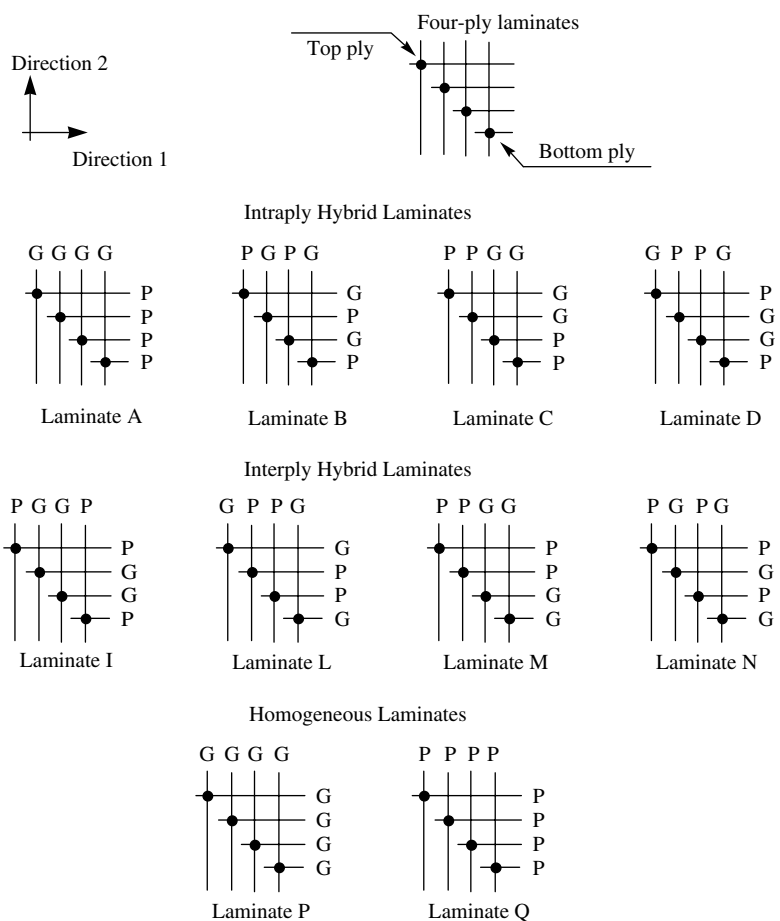


Figure 1. Schematics of the selected stacking sequences, where each fabric is identified by two perpendicular lines crossing and a point evidenced by a black circle. Letters G and P stand for glass and PVA fibres, respectively, while directions 1 and 2 represent the loading directions for the tensile tests.

Table 2. Average thickness, fibre volume fraction, density and void content data for the laminates

Laminate	Thickness (mm)	Partial fibre volume fraction along direction 1 (vol%)		Partial fibre volume fraction along direction 2 (vol%)		ρ_{th} (kg m ⁻³)	ρ_{exp} (kg m ⁻³)	Void content (%)
		E-glass	PVA	E-glass	PVA			
A	1.87 ± 0.05	0.0	34.5	17.5	0.0	1480	1470	0.68
B	1.88 ± 0.01	8.5	16.5	8.5	16.5	1460	1450	0.68
C	1.97 ± 0.03	8.5	15.5	8.5	15.5	1460	1450	0.34
D	1.83 ± 0.06	8.5	16.5	8.5	16.5	1470	1460	0.68
I	1.60 ± 0.07	9.5	14.5	9.5	6.5	1490	1480	0.34
L	1.44 ± 0.11	10.0	15.0	10.0	7.0	1500	1490	0.67
M	1.67 ± 0.03	9.0	14.0	9.0	6.0	1480	1470	0.68
N	1.58 ± 0.08	9.5	15.0	9.5	7.0	1500	1480	1.00
P	1.60 ± 0.03	20.0	0.0	20.0	0.0	1750	1730	1.14
Q	1.58 ± 0.06	0.0	30.0	0.0	14.0	1250	1250	0.00

Fibre fraction and void content measurements

The fibre content data reported in Table 2 were obtained in the following ways: (i) the fibre weight fraction (W_f) of the composites was estimated by multiplying the mass per unit area of each inserted fabric by the measured external area of the specimen and rating the obtained value to the overall weight of the specimens; (ii) the fibre volume fraction (V_f) was then obtained by considering the fibre and matrix densities reported above.

The void content of the composites was calculated according to the following equation (ASTM Standard D2734):

$$V = 100 \frac{(\rho_{th} - \rho_{exp})}{\rho_{th}} \tag{1}$$

where V is the void content (vol%), ρ_{th} the theoretical density of the composite, and ρ_{exp} the experimental value of the density measured for the composite. The

theoretical densities of the composites was estimated by using the following expression:¹²

$$\rho_{th} = \frac{1}{\frac{(1 - W_f)}{\rho_m} + \frac{W_f}{\rho_f}} \quad (2)$$

where ρ_m and ρ_f are the densities of the matrix and fibre, respectively. The experimental densities of the pure matrix and the composite specimens were measured in water at 20 °C by the displacement method, following ASTM Standard D 792.

Mechanical tests

Monotonic uniaxial tensile tests were performed by following the specifications of ASTM Standard D 3039 on rectangular specimens with an overall length of 100 mm and a width of 10 mm, along the loading directions 1 and 2 shown in Figure 1. The distance between the grips was fixed at 60 mm and all samples were tested by using an Instron 4502 tensile tester equipped with a 10 kN load cell. All tensile measurements were performed at room temperature, at a cross-head speed of 5 mm min⁻¹ on at least five specimens. In any case, the load–displacement raw data were corrected by taking into account the machine compliance, separately evaluated under the same testing configuration and conditions.

The impact behaviour was evaluated by a Charpy instrumented pendulum (CEAST model 6549) on rectangular specimens (10 mm wide and 100 mm long), with the span length fixed at 43 mm. Specimens were supported via a horizontal simple beam to the machine anvils and broken by a single swing of the pendulum, with the impact line midway between the supports. The striking nose of the pendulum was characterized by an included angle of 45 ° and the tip was rounded to a radius of 3.17 mm. All impact tests were performed under the following experimental conditions: hammer weight, 2.5 kg; striking speed, 1.513 m s⁻¹; data acquisition time, 64 ms; sampling time, 32 μs. At least six specimens were utilized for each experimental condition, and non-symmetric laminates were tested on both sides.

RESULTS AND DISCUSSION

Measurements of density were carried out in order to estimate the void content in the composites; the experimental data (ρ_{th}) were then compared with the theoretical values of density (ρ_{exp}), calculated as described in the above experimental section. As evidenced in Table 2, from comparison of ρ_{exp} and ρ_{th} , it clearly appears that the hand lay-up manufacturing process leads to a satisfactory impregnation level of the fabrics and consequently results in being effective in producing composites with a low void content (in most cases, lower than 1 %). The void content of a composite may significantly affect some of its mechanical properties: in fact, a good composite

should have less than 1 % voids, whereas a poorly made composite can have up to 5 % void content.¹²

Tensile behaviour

Typical stress–strain curves, obtained for homogeneous composites and the pure matrix, reported in Figure 2, are characterized by a monotonic load increase up to rupture. The PVA fabric homogeneous samples (Q1 and Q2) show a pronounced ‘knee’, located between 0.5 and 1.0 % strain, which is associated with the peculiar yielding behaviour of the PVA fibres used for composite manufacture, as confirmed by tensile tests performed on single PVA fibres.⁴¹ The stress–strain slope change displayed by the E-glass homogeneous sample (P1), at a strain level of about 2.0 % (which is also detectable in the Q1 sample), could be probably related to the occurrence of matrix damage, as can be hypothesized on the basis of the pure matrix stress–strain curve also reported in Figure 2. The characteristic stress–strain curves of hybrid intraply composites are reported in Figures 3a and 3b, where it can be seen how the stress–strain behaviour is strongly affected by the stacking sequence. As schematically illustrated in Figure 1, laminate type A contains only PVA fibres oriented along direction 1 and E-glass fibres along direction 2. As a consequence, the stress–strain behaviours of samples A1 and A2 (see Figure 3a) reflect those of the corresponding homogeneous composites, thus providing evidence that the presence of fibres of a different nature in the transversal direction does not substantially affects the tensile behaviour, besides the fact that a slightly higher elongation at break is observed for the hybrid composites. Intraply hybrid composites, in which both E-glass and PVA fibres are simultaneously present along the loading direction (ie laminates B, C, and D), show a more complex tensile behaviour, as characterized by a progressive failure of the various plies. In particular, for sample B2 (see Figure 3a), where PVA and E-glass fibres are alternatively stacked along the same loading direction, four following load drops can be detected: the first load drop is associated

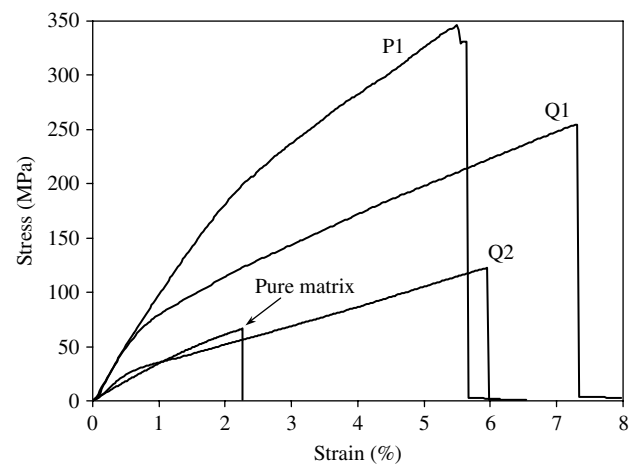


Figure 2. Stress–strain curves obtained for the homogeneous laminates (samples P1, Q1 and Q2) and the pure matrix.

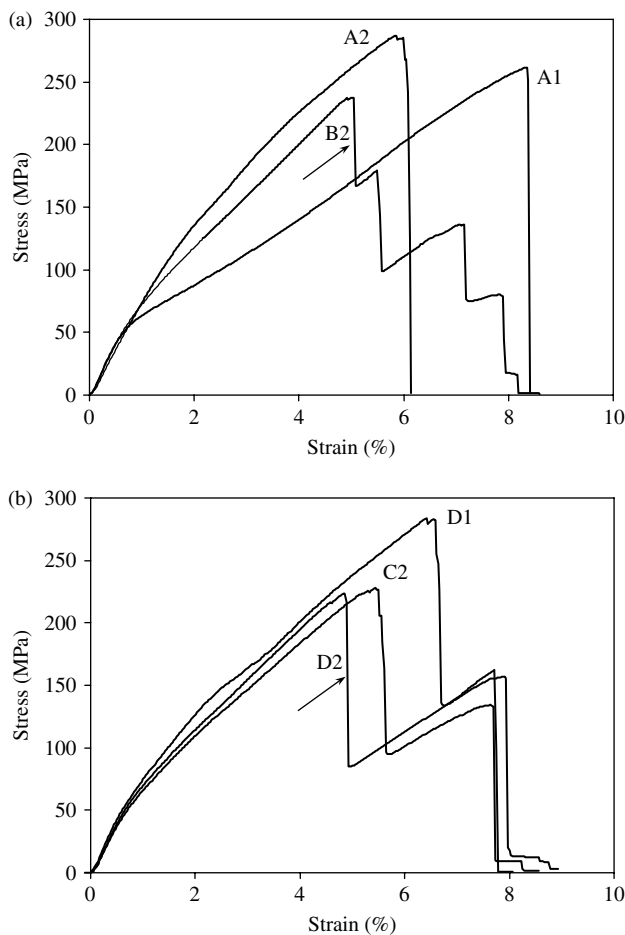


Figure 3. Stress–strain curves obtained for the intraply hybrid laminates: (a) samples A1, A2 and B2; (b) samples C2, D1 and D2.

to the failure of the external E-glass layer, the second one corresponds to the failure of the internal E-glass layer, the third one indicates failure of the external PVA layer, and the last load drop corresponds to the failure of the internal PVA layer. The lower strain at break of the external layers with respect to the internal ones is probably due to the higher probability of critical defects on the external surfaces, due to handling and sample machining, and to a more complex state of thermal stresses related to the presence of a free surface. Due to the different stacking sequence, for samples C2, D1 and D2, only two load drops can be observed, with the first one being related to the E-glass layers and the second one due to the PVA layers failure. For laminate D, it is interesting to observe that along direction 1 the first load drop occurs at high strain levels with respect to direction 2. This behaviour could probably be explained by considering that along direction 1 both of the E-glass layers are internal and consequently fail at high strain levels, with respect to direction 2, where both E-glass layers are located externally. In general, a somewhat better behaviour is evidenced by the symmetric laminates (A and D) with respect to the non-symmetric laminates (B and C), probably due to residual thermal stresses.

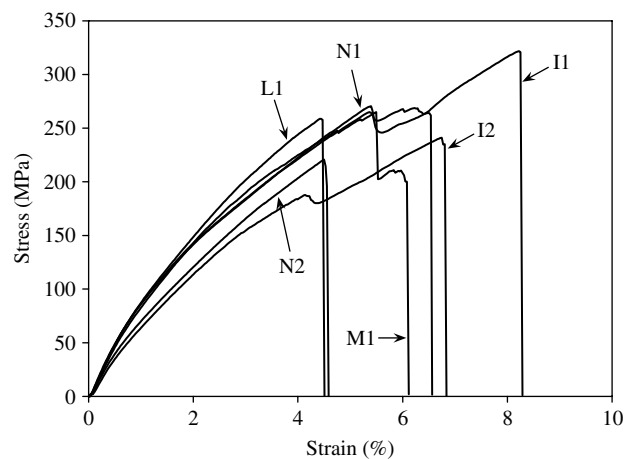


Figure 4. Stress–strain curves obtained for the interply hybrid laminates (samples I1, I2, L1, N1, N2, M1).

Typical stress–strain curves of the hybrid interply composites are reported in Figure 4. The Load drops are now not as pronounced as in the case of intraply hybrids composites. It is interesting to observe that, due to the higher PVA fibre content, sample I1 fails at a strain value higher than sample I2. A direct comparison between samples I1 and L1, characterized by an almost equal fibre volume fraction, clearly confirms that the presence of glass fibres in the external layers can be associated with the lower strain at break values. The tensile behaviour of samples M and N is quite similar. The higher strain at break of sample N1, in comparison to sample N2, can be related to the higher PVA fibre volume fraction along direction 1.

The tensile experimental data obtained for various composites and loading directions are summarized in Table 3, while Table 4 reports the specific tensile data, ie values normalized to the material density. It is important to observe that, with a proper choice of composition and stacking sequence, the E-glass/PVA hybrid composites can achieve tensile properties comparable with those of the homogeneous E-glass laminate (P1). In particular, the interply hybrid sample I1 is characterized by modulus and strength values which are essentially equal to those of the P1 sample while its elongation at break is much higher, which accounts for an improved tensile energy to break. By looking at the specific properties (Table 4), it is worth noting that most hybrid composites have specific tensile modulus and energy to break values which are comparable to, or higher than those of the homogeneous E-glass composites.

Impact performance

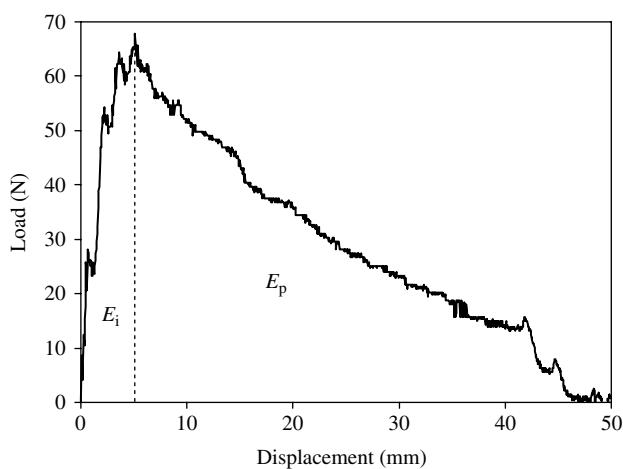
A typical load–displacement curve as obtained from the instrumented impact tests, is reported in Figure 5. For each specimen, the total impact absorbed energy (E_t) could be evaluated by measuring the total area under the curve and then normalizing this to the specimen cross-sectional area. As evidenced in Figure 5, E_t is the sum of the crack initiation energy (E_i) and the crack propagation energy (E_p). Beaumont

Table 3. Experimental data obtained from the uniaxial tensile tests on the various composites

Sample	Elastic modulus (MPa)	Maximum stress (MPa)	Strain at maximum stress (%)	Strain at break (%)	Tensile energy to break (J m^{-3})
A1	9800 ± 300	264 ± 5	8.4 ± 0.2	8.4 ± 0.2	1250 ± 40
A2	7800 ± 100	274 ± 8	5.7 ± 0.4	6.0 ± 0.6	1000 ± 100
B1 (≈B2)	9300 ± 90	237 ± 8	5.1 ± 0.3	7.9 ± 0.2	1050 ± 40
C1 (≈C2)	8600 ± 300	230 ± 10	5.4 ± 0.3	7.6 ± 0.2	970 ± 40
D1	9600 ± 200	280 ± 10	6.7 ± 0.4	7.8 ± 0.1	1290 ± 60
D2	9300 ± 100	240 ± 10	5.2 ± 0.3	8.0 ± 0.3	1100 ± 100
I1	11300 ± 200	320 ± 10	8.0 ± 0.7	8.10 ± 0.5	1630 ± 140
I2	8600 ± 100	240 ± 10	6.9 ± 0.3	6.9 ± 0.3	1000 ± 100
L1	11200 ± 700	259 ± 6	4.6 ± 0.6	4.6 ± 0.6	690 ± 60
M1	10700 ± 100	260 ± 10	5.4 ± 0.6	6.2 ± 0.2	1030 ± 80
N1	11100 ± 400	270 ± 20	5.6 ± 0.4	6.0 ± 0.7	1050 ± 150
N2	9100 ± 200	211 ± 7	4.5 ± 0.1	4.5 ± 0.1	540 ± 20
P1 (= P2)	11800 ± 200	340 ± 30	5.7 ± 0.5	5.7 ± 0.5	1200 ± 200
Q1	10700 ± 50	250 ± 10	7.5 ± 0.5	7.5 ± 0.5	1100 ± 100
Q2	5900 ± 200	125 ± 6	6.3 ± 0.4	6.3 ± 0.4	440 ± 40
Pure matrix	3500 ± 60	65 ± 9	2.2 ± 0.4	2.2 ± 0.4	80 ± 30

Table 4. Specific tensile data obtained for the various composites

Sample	Specific elastic modulus ($\text{MPa m}^3 \text{ kg}^{-1}$)	Specific maximum stress ($\text{MPa m}^3 \text{ kg}^{-1}$)	Specific energy to break (J kg^{-1})
A1	6.67 ± 0.18	0.180 ± 0.003	0.85 ± 0.03
A2	5.31 ± 0.07	0.186 ± 0.005	0.68 ± 0.07
B1 (≈B2)	6.41 ± 0.06	0.163 ± 0.006	0.72 ± 0.03
C1 (≈C2)	5.93 ± 0.21	0.159 ± 0.007	0.67 ± 0.03
D1	6.58 ± 0.14	0.192 ± 0.007	0.88 ± 0.04
D2	6.41 ± 0.070	0.166 ± 0.007	0.76 ± 0.07
I1	7.64 ± 0.14	0.216 ± 0.007	1.10 ± 0.09
I2	5.81 ± 0.07	0.162 ± 0.007	0.68 ± 0.07
L1	7.52 ± 0.47	0.174 ± 0.004	0.46 ± 0.04
M1	7.33 ± 0.07	0.178 ± 0.007	0.71 ± 0.05
N1	7.50 ± 0.27	0.182 ± 0.014	0.71 ± 0.10
N2	6.15 ± 0.14	0.143 ± 0.005	0.36 ± 0.01
P1 (= P2)	6.82 ± 0.12	0.197 ± 0.017	0.69 ± 0.12
Q1	8.56 ± 0.04	0.200 ± 0.008	0.88 ± 0.08
Q2	4.72 ± 0.16	0.100 ± 0.005	0.35 ± 0.03
Pure matrix	2.85 ± 0.05	0.053 ± 0.007	0.07 ± 0.02

**Figure 5.** A typical load–displacement curve (for sample A1) from the instrumented impact test, displaying the energy partition between crack initiation (E_i) and crack propagation (E_p) contributions.

*et al*¹³ defined a dimensionless parameter, known as the ductility index (DI), which has been found useful for ranking the impact performance of different materials under similar testing conditions. The DI is defined as the ratio between the propagation energy and the initiation energy, as follows:

$$DI = \frac{E_p}{E_i} \quad (3)$$

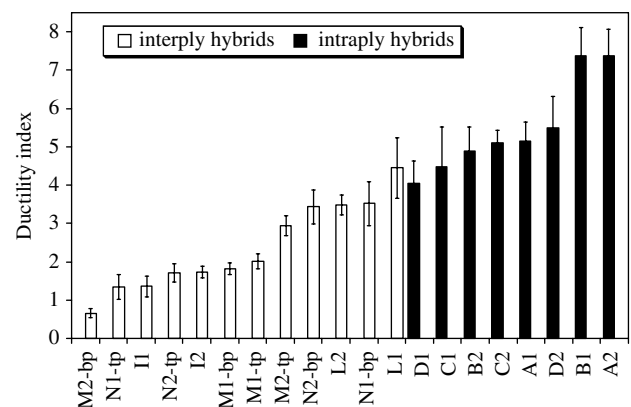
High values of DI would mean that most of the total energy is expended in crack propagation. The total impact energy, specific total impact energy and ductility index data for the various composites, impacted on the top and bottom surfaces, are summarized in Table 5. The homogeneous E-glass laminate shows a specific total impact energy of 64 J m kg^{-1} , while for the homogeneous PVA laminate specific impact energies of 72 and 46 J m kg^{-1} were

Table 5. Impact data obtained for the various composites

Sample	Impacted side	Total impact energy (kJ m ⁻²)	Specific total impact energy (J m kg ⁻¹)	Ductility index
A1	Top ply	90 ± 6	61 ± 4	5.15 ± 0.50
A2	Top ply	79 ± 2	54 ± 1	7.38 ± 0.68
B1	Top ply	89 ± 5	61 ± 3	7.37 ± 0.75
B2	Top ply	96 ± 3	66 ± 2	4.89 ± 0.63
C1	Top ply	92 ± 8	63 ± 6	4.47 ± 1.04
C2	Top ply	103 ± 3	71 ± 2	5.10 ± 0.32
D1	Top ply	91 ± 4	62 ± 3	4.05 ± 0.59
D2	Top ply	85 ± 5	58 ± 3	5.50 ± 0.81
I1	Top ply	89 ± 7	60 ± 5	1.36 ± 0.27
I2	Top ply	66 ± 4	45 ± 3	1.73 ± 0.16
L1	Top ply	99 ± 10	66 ± 7	4.45 ± 0.79
L2	Top ply	96 ± 7	64 ± 5	3.48 ± 0.26
M1	Top ply	108 ± 8	73 ± 5	2.01 ± 0.19
M1	Bottom ply	67 ± 3	46 ± 2	1.82 ± 0.16
M2	Top ply	89 ± 2	61 ± 1	2.95 ± 0.26
M2	Bottom ply	45 ± 5	31 ± 3	0.66 ± 0.11
N1	Top ply	111 ± 11	75 ± 7	1.34 ± 0.32
N1	Bottom ply	84 ± 4	57 ± 3	3.52 ± 0.58
N2	Top ply	93 ± 5	63 ± 3	1.71 ± 0.20
N2	Bottom ply	68 ± 6	46 ± 4	3.43 ± 0.45
P1 (= P2)	Top ply	111 ± 8	64 ± 5	3.90 ± 0.54
Q1	Top ply	90 ± 10	72 ± 8	2.19 ± 0.47
Q2	Top ply	58 ± 6	46 ± 5	3.26 ± 1.04
Pure matrix	—	6 ± 2	5 ± 2	0

measured for directions 1 and 2, respectively. The specific total impact energy for the intraply composites ranges from 54 to 71 J m kg⁻¹, depending on the stacking sequence and testing direction. The interply composites, impacted on the top ply, show specific total impact energy values in the range 45 to 75 J m kg⁻¹, while lower values, from 31 to 57 J m kg⁻¹, were measured for non-symmetric interply composites impacted on the bottom ply. In fact, the impact performances of non-symmetric laminates are strictly related to the stacking sequence with respect to the impact side:²⁸ in general, higher total impact energy values were measured for interply laminates where the outer layers are of E-glass type. Similar comments can be extended to the specific total impact energy values; for a few samples (C2, M1 top ply and N1 top ply), the specific total energy is significantly higher than that of the homogeneous E-glass laminate.

In Figure 6, the ductility indices are reported in ascending order for both intraply and interply composites. It is interesting to observe that hybrid intraply composites show higher ductility index values than those of the interply hybrid composites. This behaviour is indicating an higher efficiency in hindering the crack propagation when E-glass and PVA fibres are intimately mixed in the same layer with respect to the case in which they are located in separated plies. Moreover, as evidenced in Table 5, all hybrid intraply composites are characterized by ductility index values superior to those of homogeneous laminates (P1, Q1 and Q2).

**Figure 6.** Ductility index values for interply and intraply hybrid composites, reported in ascending order.

CONCLUSIONS

The tensile and impact mechanical properties of intraply and interply hybrid composites, based on E-glass and poly(vinyl alcohol) fabrics, have been investigated. The stress–strain curves appear to be markedly affected by the plies stacking sequences and the loading directions. It is interesting to note that, through an appropriate laminate design, the E-glass/PVA hybrids could achieve specific tensile properties comparable to or higher than those of the homogeneous E-glass laminate, with an improved elongation at break. In particular, better tensile performances were achieved from symmetric interply hybrids with internal E-glass layers.

Impact data clearly show that hybrid intraply composites reached higher ductility index values

when compared to those of interply hybrids and homogeneous composites, probably due to the higher efficiency in hindering crack propagation in the case of E-glass and PVA fibres intimately mixed in the same layer.

ACKNOWLEDGEMENTS

The authors wish to thank Dr Lino Credali for helpful suggestions and discussion of the results, and Mr Andrea Bassi for his contribution to many aspects of the experimental work. Fibre e Tessuti Speciali Srl (FTS) (Turin, Italy) and SIR Industriale Spa (Milan, Italy) are kindly acknowledged for provision of the fabrics and UP resin, respectively.

REFERENCES

- 1 Short D and Summerscales J, *Composites* **10**:215–221 (1979).
- 2 Short D and Summerscales J, *Composites* **11**:33–38 (1980).
- 3 Hancox NL, *Fiber Composite Hybrid Materials*, Applied Science, London (1981).
- 4 Kretsis G, *Composites* **18**:13–23 (1987).
- 5 Richardson T, *Composites: A Design Guide*, Industrial Press Inc, New York, pp 103–104 (1987).
- 6 Bunsell AR and Harris B, *Composites* **5**:157–164 (1974).
- 7 Lowell DR, *Reinforced Plast*: 216–221 (1978).
- 8 Lowell DR, *Reinforced Plast*: 252–256 (1978).
- 9 Summerscales J and Short D, *Composites* **9**:157–166 (1978).
- 10 Manders PW and Bader MG, *J Mater Sci* **16**:2233–2242 (1981).
- 11 Sonparote PW and Lakkad SC, *Fibre Sci Technol* **16**:309–312 (1982).
- 12 Agarwal DB and Broutman JL, *Analysis and Performance of Fiber Composites*, 2nd Edn, Wiley, New York (1990).
- 13 Beaumont PWR, Reiwald PG and Zweben C, *ASTM STP* **568**:134–158 (1974).
- 14 Dorey G, Sidey GR and Hutchings J, *Composites* **9**:25–32 (1978).
- 15 Fisher S and Marom G, *Compos Sci Technol* **28**:291–314 (1987).
- 16 Aronhime J, Harel H, Gilbert A and Marom G, *Compos Sci Technol* **43**:105–116 (1992).
- 17 Jang BZ, Chen LC, Wang CZ, Lin HT and Zee RH, *Compos Sci Technol* **34**:305–335 (1989).
- 18 Peijs AAJM and Lemstra PJ, Hybrid composites based on polyethylene and carbon fibres Part1: Compressive and impact behaviour, in *Integration of Fundamental Polymer Science and Technology*, Vol 3, ed by Lemstra PJ and Kleintjens LA, Elsevier Applied Science, London, pp 218–227 (1989).
- 19 Peijs AAJM, Catsman P, Govaert LE and Lemstra PJ, *Composites* **21**:513–521 (1990).
- 20 Peijs AAJM, Venderbosch RW and Lemstra PJ, *Composites* **21**:522–530 (1990).
- 21 Peijs AAJM and Venderbosch RW, *J Mater Sci Lett* **10**:1122–1124 (1991).
- 22 Peijs AAJM and Van Klinken EJ, *J Mater Sci Lett* **10**:520–522 (1992).
- 23 Peijs AAJM and DeKok JMM, *Composites* **24**:19–32 (1993).
- 24 Jang J and Moon S, *Polym Compos* **16**:325–329 (1995).
- 25 Li Y, Xian XJ, Choy CL, Guo M and Zhang Z, *Compos Sci Technol* **59**:13–18 (1999).
- 26 Park R and Jang J, *Compos Sci Technol* **58**:1621–1628 (1998).
- 27 Wu Y, Zhong WH, Sun ZJ, Torki A and Zhang ZG, *J Mater Sci Technol* **18**:357–360 (2002).
- 28 Schrauwen B, Bertens P and Peijs T, *Polym Polym Compos* **10**:259–272 (2002).
- 29 Mishra S, Mohanty AK, Drzal LT, Misra M, Parija S, Nayak SK and Tripathy SS, *Compos Sci Technol* **63**:1377–1385 (2003).
- 30 Kalaprasad G, Mathew G, Pavithran C and Thomas S, *J Appl Polym Sci* **89**:432–442 (2003).
- 31 Kalaprasad G and Thomas S, *J Appl Polym Sci* **89**:443–450 (2003).
- 32 Thwe MM and Liao K, *Plast Rubber Compos* **31**:422–431 (2002).
- 33 Marom G, Fischer A, Tuler FR and Wagner HD, *J Mater Sci* **13**:1419–1426 (1978).
- 34 Zeng QD and Lin XH, *Acta Mechan Solid Sin* **16**:33–40 (2003).
- 35 Carter GB and Schenk VTJ, Ultra-high modulus organic fibres, in *Structure and Properties of Oriented Polymers*, ed by Ward IM, Applied Science Publishers, London, pp 454–492 (1975).
- 36 Lemstra PJ and Kirshbaum R, *Polymer* **26**:1372–1384 (1985).
- 37 Peijs T, van Vught RJM and Govaert LE, *Composites* **26**:83–90 (1995).
- 38 Govaert LE and Peijs T, *Polymer* **36**:3589–3592 (1995).
- 39 Sakurada I, *Poly(vinyl alcohol) Fibres*, Marcel Dekker, New York, pp 103–104, 361–395 (1985).
- 40 Sakurada I and Okaya T, Vinyl fibers, in *Handbook of Fiber Chemistry*, 2nd Edn, ed by Lewin M and Pearce EM, Marcel Dekker, New York, pp 279–354 (1998).
- 41 Pegoretti A, unpublished results.